Izvestiya Vysshikh Uchebnykh Zavedeniy. Applied Nonlinear Dynamics. 2022;30(2)

Article
DOI: 10.18500/0869-6632-2022-30-2-208-232

Simple and complex dynamics in the model of evolution of two populations coupled by migration with non-overlapping generations

M. P. Kulakov✉, *E. Ya. Frisman*

Institute for Complex Analysis of Regional Problems,
Far Eastern Branch, Russian Academy of Sciences, Birobidzhan, Russia
E-mail: ✉k_matvey@mail.ru, frisman@mail.ru
Received 6.02.2022, accepted 1.03.2022, published 31.03.2022

Abstract. *Purpose* is to study the mechanisms leading to genetic divergence (stable genetic differences between two adjacent populations). We considered the following classical model situation. Populations are panmictic with Mendelian rules of inheritance. The action of natural selection (differences in fitness) on each of population is the same and is determined by the genotypes of only one diallel locus. We assume that adjacent generations do not overlap and genetic transformations can be described by a discrete time model. This model describes the change in the concentration of one of the alleles in each population and the ratio (weight) of first population to the total size. *Methods.* We used the analogue of saddle charts to construct parametric portraits showing the domains of qualitatively different dynamic modes. The study is supplemented with phase portraits, basins of attraction and bifurcation diagrams. *Results.* We found that the model dynamic regimes qualitatively coincide with the regimes of a similar model with continuous time, but only for a weak migration. With a strong coupling, fluctuations of the phase variables are possible. We showed that the genetic divergence is possible only with reduced fitness of heterozygotes and is the result of a series of bifurcations: pitchfork bifurcation, period doubling, or saddle-node bifurcation. After these qualitative changes, the dynamics become bi- or quadstable. In the first case, the solutions corresponding to the genetic divergence are unstable and are just a part of the transient process to monomorphic state. In the second case, the divergence is stable and appears as 2-cycle for a strong migration coupling. *Conclusion.* In neighboring populations, movement towards an asymptotic genetic structure (monomorphism, polymorphism or divergence) can be strictly monotonous or in the form of damped unstable or undamped stable fluctuations with a period of 2 for biologically significant parameters. For insignificant parameters, we found a complex dynamics (chaos) that consist of divergent fluctuations around fixed points and quasi-random transitions between them.

Keywords: genetic divergence, discrete time model, dynamics, bifurcations, fluctuations, bi- and quad-stability.

Acknowledgements. This work was carried out within the framework of the state targets of the Institute for Complex Analysis of Regional Problem of the Far Eastern Branch of the Russian Academy of Sciences.

For citation: Kulakov MP, Frisman EYa. Simple and complex dynamics in the model of evolution of two populations coupled by migration with non-overlapping generations. Izvestiya VUZ. Applied Nonlinear Dynamics. 2022;30(2):208–232. DOI: 10.18500/0869-6632-2022-30-2-208-232

Introduction

The theoretical study of the evolution and microevolution of biological populations under the influence of natural selection has a long and rich history [1–3]. One of the most interesting tasks is related to the search for the basic mechanisms of speciation, and its complexity is determined by the following circumstances. On the one hand, under the action of selection in the population

is the consolidation (fixation) of such a trait (genotype), which provides the greatest fitness of individuals and, as a result, the highest reproduction rate. As a result , in isolated in populations, such a genotype is fixed, and others disappear or dissolve among heterozygotes, and there is no subsequent evolution preceding a new one speciation does not occur. On the other hand, in the presence of geographical isolation, pronounced hereditary differences may occur between initially genotypically similar aggregates of individuals (populations): primary genetic divergence.

It is important to understand under what conditions the primary genetic divergence will be stable and will persist if spatial isolation between populations is violated.

This task has been considered by many researchers [4–7]. It has been shown that in order to achieve divergence between different populations, only only genetic mechanisms — still need a strong ecological mechanism that provides regulation of population growth and significantly affects evolutionary processes. In addition, genetic and ecological processes should operate at comparable speeds [8, 9]. Growth restrictions may be related to various mechanisms of self-imitation within the population [10–13] or interspecific interactions [14–16]. Apparently, this is also true for the more general case when selection is based on two or more traits (genotype) [17–19].

This work continues the description of the mechanisms and the study of the conditions for the occurrence of primary genetic divergence, which was started in [20]. A discrete-time mathematical model based on recurrent equations (maps) and describing the change in allele frequencies and the ratio of numbers in the system of two adjacent panmictic populations associated with migration is considered. From a meaningful, biological point of view, discrete-time models are more adequate than models based on differential equations, in cases where Populations of biological species with a fixed breeding season occupying a very short life cycle period are considered [21]. In particular, this is usually characteristic of species with pronounced stages of development, metamorphosis and non-overlapping generations, when all the individuals involved in breeding do not survive until the next breeding season.

In this paper, the possibilities, conditions and mechanisms of the formation of a stable difference in the genetic structures of the populations under consideration are investigated by the methods of bifurcation analysis. The model under study, being a discrete analog models from the work [20], has a number of dynamics features related to fluctuations and complex modes (chaos). Their research, to some extent, it goes beyond the scope of the substantive part of the problem, but it may be interesting for specialists in the theory of dynamical systems.

1. Brief description of the model

As in the previous work [20], we will limit ourselves to describing the simplest situation when all diversity in a population is determined by a single diallel locus with allelomorphs A and a. To describe the action of natural selection each genotype — AA, Aa and aa — can be matched with one coefficient w_{AA}, w_{Aa} and w_{aa}, called fitness. This coefficient is equal to half the ratio of the number of gametes that entered the zygotes of descendants of this genotypic class, survivors and those who have started migration and gametoproduction (reproduction), to the total number of organisms born of this genetic class. Assume that there is local panmixia, that is, free crossing of individuals with different genotypes occurs in each population. It is easy to show that in the case of panmixia, to describe the dynamics of the genetic structure of a local population, it is enough to monitor a single value of q — the concentration of gametes carrying, for example, the allele A, since between the concentrations of fertilized zygotes (individuals), bearing the genotypes AA, Aa and aa, and the concentrations of alleles A and a present in the gametes of individuals that formed them, in this case, the relations following from the Hardy-Weinberg law are fulfilled.

In the case of a local population with disjoint generations, the concentration of gametes with the A allele, as well as the total number of N of the population, are determined by the following classical equations [4–6], which relate their values in adjacent generations:

$$\begin{cases} q(t+1) = q_n\Big(w_{AA}q(t) + w_{Aa}\big(1-q(t)\big)\Big)/\bar{w}(t), \\ N(t+1) = \bar{w}(t)N(t), \end{cases} \tag{1}$$

where $t = 0, 1, 2, \ldots$ — generation number, $\bar{w}(t) = w_{AA}q^2(t) + 2w_{Aa}q(t)(1-q(t)) + w_{aa}(1-q(t))^2$ — average fitness of the population. The first equation of the system (1) does not depend on the second and describes the change in the concentration of the allele A under the action of natural selection. Different ratios of the parameters w_{AA}, w_{Aa} and w_{aa} defines a specific type of selection in the population. Since the model is sufficiently aggregated, it is not so important to understand the qualitative properties of the model (1) as the absolute values of the parameters, but their ratio. In the case of the so -called driving selection $w_{AA} > w_{Aa} > w_{aa} > 0$ ($w_{aa} > w_{Aa} > w_{AA} > 0$) only the fixed point $\bar{q} = 1$ is stable ($\bar{q} = 0$). There are no other fixed points. As a result , the concentration of the A allele increases (decreases) according to the logistic law, from any initial state $0>q(0)>1$, linebreak and only homozygotes with AA (aa) alleles remain in the population, and the second homozygotes and heterozygotes inevitably die. In the case when the fitness of heterozygotes lies outside the range adaptations of homozygotes, between fixed points 0 and 1 appears additional point $q^* = (w_{aa} - w_{Aa})/(w_{AA} - 2w_{Aa} + w_{aa})$. With $w_{Aa} > w_{AA}$ and $w_{Aa} > w_{aa}$ it is stable, and over time , a stable polymorphism is established in the population, in which all three genotypes coexist with a constant value of both their concentrations and frequencies of alleles of their components. With $w_{Aa} < w_{AA}$ and $w_{Aa} < w_{aa}$, the point q^* — is unstable. In the latter case, at $0 > q(0) > q^*$, the frequency of the A allele drops to 0, and at $q^* > q(0) > 1$ grows to 1. However, polymorphism in this case can persist in the population for quite a long time (during transition process) if $q(0)$ is close to q^* (but strictly not equal to this value).

In any of these three cases, the average fitness of $\bar{w}(t)$ can only grow as the genetic structure (the value of $q(t)$) will tend to one of the possible stationary states (fixed points 0, 1 or $0 < q^* < 1$). At the beginning of this growth, fitness, as a rule, does not exceed one. As a result, at certain values of $N(0)$, the number of $N(t)$ in the model (1) may fall so much that it reaches zero, while q will continue to rise or fall. Obviously, the model (1) loses its meaning here. However, earlier it may happen that the value of $\bar{w}(t)$ will reach one and the decline in numbers will stop. Or from some number of the season t, the value of $\bar{w}(t)$ will exceed one, and the fall will be replaced by exponential growth. Having reached the final genetic structure (the limit value of $q(t)$ at $t \to \infty$), fitness also reaches its limit value, depending on which limit state is stable: $\bar{w}(t) \to w_{aa}$ if $q(t) \to 0$; $\bar{w}(t) \to w_{AA}$, if $q(t) \to 1$; $\bar{w}(t) \to (w_{AA}w_{aa} - w_{Aa}^2)/(w_{AA} - 2w_{Aa} + w_{aa})$ if $q(t) \to q^*$. Obviously, the absolute values of the parameters w_{AA}, w_{Aa} and w_{aa} are already important here, as well as the initial genetic structure and starting number $q(0)$ и $N(0)$.

Let us now consider two such adjacent populations that exchange migrants with the intensity of migration flows proportional to the size of the population from which these migrants originate. The proportionality coefficient or, in other words, the migration coefficient m is the same for all genotypes in both populations. In this case, the following sequence of population processes is possible: formation of zygotes from gametes, mortality or selection of zygotes, migration between populations after selection, production of new gametes. Let's limit ourselves to the case when both populations identical in terms of fitness values of w_{AA}, w_{Aa} and w_{aa}, as well as gametoproducts. Let's assume that heterozygotes produce the same number of gametes of each type, there is no differentiation of gamete survival, and gametoproduction is calculated taking into account the

loss of gametes. By describing these processes through changes in the numbers of gametes and zygotes at different stages of population development, we can obtain the following system of recurrent equations with four variables:

$$\begin{cases} q_1(t+1) = & \dfrac{1}{G_1(t)}\Bigg((1-m)q_1(t)\Big(w_{AA}q_1(t)+w_{Aa}\big(1-q_1(t)\big)\Big)+ \\ & \qquad + m\dfrac{1-p(t)}{p(t)}q_2(t)\Big(w_{AA}q_2(t)+w_{Aa}\big(1-q_2(t)\big)\Big)\Bigg), \\ q_2(t+1) = & \dfrac{1}{G_2(t)}\Bigg((1-m)q_2(t)\Big(w_{AA}q_2(t)+w_{Aa}\big(1-q_2(t)\big)\Big)+ \\ & \qquad + m\dfrac{p(t)}{1-p(t)}q_1(t)\Big(w_{AA}q_1(t)+w_{Aa}\big(1-q_1(t)\big)\Big)\Bigg), \\ p(t+1) = & \dfrac{G_1(t)}{G(t)}p(t), \\ N(t+1) = & G(t)N(t), \end{cases} \tag{2}$$

p q_1 and q_2 — concentrations of the A allele in the first and second populations ($0 \leqslant q_i \leqslant 1$), $p = N_1/(N_1+N_2)$ — weight of the first population ($0 < p < 1$), $N = N_1 + N_2$ — the number of both populations in the tth season. Coefficients $G_1(t) = (1-m)\bar{w}_1(t) + m\dfrac{1-p(t)}{p(t)}\bar{w}_2(t)$, $G_2(t) = (1-m)\bar{w}_2(t) + m\dfrac{p(t)}{1-p(t)}\bar{w}_1(t)$ and $G(t) = p(t)G_1(t) + (1-p(t))G_2(t) = p(t)\bar{w}_1(t) + (1-p(t))\bar{w}_2(t)$ are equal to the average generalized fitness of the first, second, and overall of the entire system populations where $\bar{w}_i = w_{AA}q_i^2(t) + 2w_{Aa}q_i(t)(1-q_i(t)) + w_{aa}(1-q_i(t))^2$ ($i = 1, 2$). The model (2) represents two interconnected systems (1) with a variable migration coefficient. Due to the independence of the concentrations of q_i and the weight of p from the total number, we can limit ourselves to considering only the first three equations.

It should be noted that in the traditional approach, when describing the dynamics of allele frequencies, the number as a variable is not often used. It is believed that there are quite a lot of individuals and selection does not significantly change the total number — only the ratio of genotypes changes. For example, the articles [10, 22] consider a similar model situation, but the number is considered as a parameter, the variation of which changes the area of monomorphism and polymorphism in adjacent populations. Using population size or weight complicates the model compared to the models in these two papers — in (2) the coupling coefficient turns out to be a variable. It is easy to show that in the case of synchronous monotonic growth of both populations ($p = 1/2$) qualitatively, the behavior of the system (2) and the models from these works will coincide. For the sake of completeness of the study, this case is considered in the last paragraph of the article.

It is also important to emphasize here that the model (2) corresponds to the situation when migration occurs after selection in the specified chain of population processes . We can also consider the case when migration precedes selection. However, it is not difficult to show that the model equations in the case of the same selection in adjacent populations does not depend on the sequence of these population processes and in these situations completely coincide [6].

We specify the type of selection. We are interested in the possibility and conditions for the formation of genetic divergence (stable differences in genetic structures) in the system of two adjacent populations living in a homogeneous area. The question arises: what type of selection

can lead to genetic divergence? Driving selection, when $w_{AA} > w_{Aa} > w_{aa}$ or $w_{aa} > w_{Aa} > w_{AA}$, is clearly not suitable here. So it is necessary to analyze the situation when the fitness of a heterozygote lies outside the range of adaptations of homozygotes. Let us confine ourselves to consideration «symmetric» case $w_{AA} = w_{aa}$ and, since without taking into account the equation, describing the dynamics of the number, only the ratios of these parameters are important, let's assume that $w_{AA} = w_{aa} = 1$, $w_{Aa} = 1 + s > 0$, where $s > -1$ — the selection coefficient for heterozygote [10, 22, 23]. Given this, we rewrite the equations (2) as follows:

$$\begin{cases} q_1(t+1) = \dfrac{1}{G_1(t)}\Bigg(\big(1-m\big)q_1(t)\Big(1+s\big(1-q_1(t)\big)\Big)+ \\ \qquad\qquad + m\dfrac{1-p(t)}{p(t)}q_2(t)\Big(1+s\big(1-q_2(t)\big)\Big)\Bigg), \\ q_2(t+1) = \dfrac{1}{G_2(t)}\Bigg(\big(1-m\big)q_2(t)\Big(1+s\big(1-q_2(t)\big)\Big)+ \\ \qquad\qquad + m\dfrac{p(t)}{1-p(t)}q_1(t)\Big(1+s\big(1-q_1(t)\big)\Big)\Bigg), \\ p(t+1) = \dfrac{G_1(t)}{G(t)}p(t). \end{cases} \tag{3}$$

Here the average fitness is equal to the following values: $G_1(t) = (1-m)(1+2sq_1(t) \times \times (1-q_1(t))) + m\dfrac{1-p(t)}{p(t)}(1+2sq_2(t)(1-q_2(t)))$, $G_2(t) = (1-m)(1+2sq_2(t)(1-q_2(t))) + + m\dfrac{p(t)}{1-p(t)}(1+2sq_1(t)(1-q_1(t)))$ и $G(t) = 1+2s(p(t)q_1(t)(1-q_1(t))+(1-p(t))q_2(t)(1-q_2(t)))$. The number, as before, can be found from the equation: $N(t+1) = G(t)N(t)$. For biological reasons , it makes sense to talk only about those solutions of the system (3) that lie entirely in the unit cube: $0 \leqslant q_1 \leqslant 1$, $0 \leqslant q_2 \leqslant 1$ и $0 < p < 1$.

For the model (3), the most interesting case is $s < 0$, since each individual of its the equation, like the local model (1), turns out to be bistable. As a result , in the case of complete isolation ($m = 0$), different territories may persist significant differences in the genetic structure (divergence) — on one there are individuals with the A allele, on the other — with the a allele. A question arises. What are the conditions for the existence and maintenance of differences in the case of a non-zero migration relationship between populations? Are there any significant differences from the case continuously the developing population considered in the previous work [20]? To find the answer, we will perform a qualitative study of the system (3).

To begin with, we note that it is necessary to consider only the case of $s \geqslant -1$ in a meaningful way. Because otherwise the fitness of w_{Aa} for heterozygotes will be a negative value. As a result, there may be a situation in which the abundance (weight) or concentration of the A allele may reach negative values or experience fluctuations that go beyond the limits of a single cube. However, as will be shown below, even with $-2 < s < -1$, it is not difficult to find limited solutions of the system (3) that they lie entirely in a single cube and, at first glance, do not contradict the biological content. This becomes possible due to the relationship between populations, when negative values of allele frequencies in one site are «compensated» by migration influx from another site, and the final frequency turns out to be positive. For a complete understanding of the behavior solutions of the system (3) we will consider not only the biologically significant range of values of the selection coefficient $s \geqslant -1$, but also the values of $s < -1$, at which, in particular, irregular dynamics occurs.

2. Research on the sustainability of solutions

Despite the cumbersome appearance of the system (3), it is possible to perform a fairly complete study of the stability of each fixed point, including calculating the eigenvalues of the Jacobi matrix at each of the points, determining the areas of their existence and describing the mechanisms for the formation of different dynamic modes.

The system (1) has the following fixed points:

- $E_0\,(0,0,1)$ — both populations are represented only by individuals with the aa genotype (the AA or Aa genotype is missing) (monomorphic population);
- $E_1\,(1,1,1)$ — both populations consist only of individuals with the AA genotype (monomorphic population);
- $E_2\,(1/2,1/2,1/2)$ — both populations include individuals all genotypes at the same concentration of each of the two alleles (polymorphic population);
- pair of dots $E_{3,4}\left(\frac{1}{2}\pm\frac{\sqrt{s^2+4ms}}{2s},\frac{1}{2}\mp\frac{\sqrt{s^2+4ms}}{2s},\frac{1}{2}\right)$, which exists at $s<0$ and $s+4m<0$. For $s>0$, it exists for any $0\leqslant m\leqslant 1$, but lies outside the unit cube, which contradicts the meaning phase variables. A pair of dots is born (or disappears) on the line $m=-s/4$ E_3 and E_4 due to fork bifurcation. In this case, the point E_1 «splits» into a pair of points $E_{3,4}$. Each of these points corresponds to a divergent state of the population system (different alleles predominate in each population). However, as in the case of a continuous-time model, they are unstable at any parameter values.

To study the general nature of the dynamics, consider the value $Q(t)=q_1(t)p(t)+q_2(t)(1-p(t))$, which is equal to the concentration of the A allele in both populations. Substituting the right parts of the system (3) into this expression and giving similar terms, we obtain a non-autonomous recurrent equation:

$$Q(t+1)=\frac{1}{G(t)}\left(Q(t)+\frac{G(t)-1}{2}\right). \tag{4}$$

The increment of Q is equal to:

$$\Delta Q=Q(t+1)-Q(t)=\frac{G(t)-1}{G(t)}\left(\frac{1}{2}-Q(t)\right).$$

Thus, the mapping (4) has a fixed point $Q=1/2$ (for $\Delta Q=0$). This means that in the phase space of the system (3) the expression $Q=1/2$ defines a surface that turns out to be invariant with respect to the mapping (3) (mapped to itself). Then all the trajectories whose beginnings lie on this surface belong entirely to it.

It is easy to make sure that the points E_2, E_3 and E_4 belong to the surface $Q=1/2$. The stability of fixed points and the nature of global dynamics are closely related to the properties of this surface. It is easy to show that for $s>0$ the inequality $0\leqslant\frac{G-1}{G}<1$ holds, then the surface $Q=1/2$, like the point E_2, is attractive. W $-2<s<0$ is in progress $-1<\frac{G-1}{G}\leqslant 0$, then the surface $Q=1/2$ is a repulsive separatrix surface dividing the unit cube into two equal basins of attraction of stable points E_0 and E_1. Let 's denote this surface as W^S.

To understand the nature of the movement of various trajectories , consider the local stability of each of the fixed points of the system (3), which is determined by the values of the eigenvalues of the Jacobi matrix calculated at each fixed point (multipliers λ_i). In Fig. 1 shows the

arrangement of eigenvalues revealed for the system (1) relative to the unit circle. It is established that the system (1) has only real eigenvalues, which, apparently, is also true for multiple periodic points arising in the system (3) (in fig. 1 only a pair is shown $2P_{1,2}$).

Numerical analysis of the stability of fixed points with variation of the parameter s from -2 to 2 and m from 0 to 1 revealed 11 combinations of stability types of fixed points (drain, source or saddle with different numbers of stable and unstable proper subspaces). In this range of parameters, at least one point is stable (in Fig. 1 this corresponds to the selected cell): at

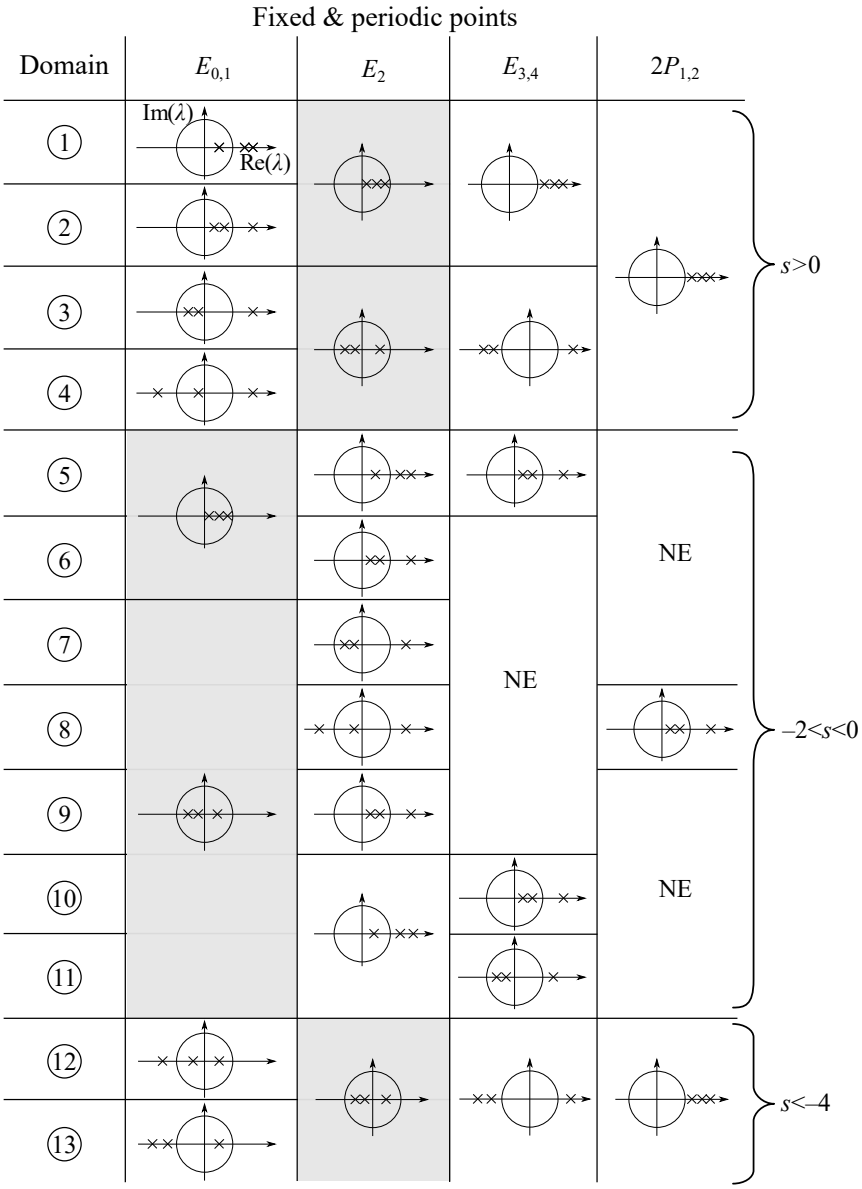

Fig. 1. Расположение собственных чисел неподвижных (E_i) и периодических точек ($2P$) относительно единичной окружности в разных областях на параметрическом портрете. Для пар $E_{0,1}$, $E_{3,4}$ и $2P_{1,2}$ значения собственных чисел совпадают, выделенная клетка — точка (или пара точек) устойчива, NE — точка не существует

Fig. 1. Location of eigenvalues on a unit circle for fixed (E_i) and periodic points ($2P$) in different domains of the parametric portrait. For couples $E_{0,1}$, $E_{3,4}$ and $2P_{1,2}$, the eigenvalues are the same. The highlighted cell corresponds to a stable point or a pair of points. NE is point does not exist

$s > 0$, the point E_2 is stable, at $-2 < s < 0$ — the point E_0 and E_1. At $-4 \leqslant s \leqslant -2$ there are no stable points in the system (3), and complex dynamics are observed. U$s < -4$ stable points reappear, and two more are added to the 11 combinations of stable and unstable points (areas *12* and *13* in Fig. 1). Each of these combinations is preserved at a certain ratio of parameters s and m. As a result, 13 regions can be distinguished on the parameter plane, characterized by a certain ratio of stable and saddle fixed points (analogous to saddle maps [24]). It can be argued that qualitatively equivalent types of dynamics are formed in each of these areas. In Fig. 1 and 2, *a* these parameter areas are indicated by circles with numbers *1–13*.

2.1. Simple dynamics modes. Let us consider the areas of stability and the simple dynamics modes arising in them.

In the areas *1–4*, only the point E_2 is stable, the rest are — saddles. As can be seen from Fig. 1, these regions differ in the dimension of stable and unstable proper subspaces (manifolds) in the neighborhood of each of the fixed points (see Fig. 1). For example, in the regions *1* and *4*, the saddle points E_0 and E_1 have a one-dimensional stable manifold (one eigenvalue lies inside the unit circle), and in the regions *2* and *3* — a two-dimensional stable manifold (two the eigenvalues lie inside the unit circle). But their more significant difference is that as soon as the migration parameter m turns out to be greater than 1/2 (but not more than 1), some of the eigenvalues of the Jacobi matrix (multiplier λ_i) turn out to be negative, and this happens simultaneously with all fixed points. As a result, dynamic modes arise for parameters from the *3* domain, in which the striving for a single stable point E_2 is accompanied by damping oscillations around it (see Fig. 2, *c*). At the same time the trajectory remains strictly on one side of the surface $Q = 1/2$. In the area *4* , the damped oscillations around the point E_2 are preceded by a monotonous movement in its side, combined with divergent oscillations, if the initial conditions are taken in the vicinity of unstable points E_0 or E_1. The nature of these fluctuations is clearly visible in the variable p (Fig. 2, *e*). Otherwise , there are no fluctuations, and only a monotonous movement to the point E_2 is observed. It is important to emphasize that these fluctuations, if they occur, never go beyond the limits of a single cube, unlike similar fluctuations in other areas at $s < 0$. In addition, in the areas of *1–4* the fixed points E_3 and E_4, which correspond to genetic divergence, lie outside the unit cube and are unstable nodes (sources).

In contrast to this situation in the areas *12* and *13*, as well as in the area *4* at $s < -4$ (topologically equivalent to the area *4* for $s > 0$) the points E_3 and E_4, as well as the periodic points $2P_{1,2}$ lie in the unit cube. For $0 \leqslant m < 0.5$, the points $2P_{1,2}$ lie on the line $q_1 = 1 - q_2$, $p = 0.5$ between the points E_3 and E_4, and at $0.5 < m \leqslant 1$, the points E_3 and E_4 lie between $2P_{1,2}$. As a result, there is a situation where damped oscillations are almost always they go beyond the limits of a single cube. Moreover, in these areas, the trajectory periodically it turns out to be on different sides of the surface $Q = 1/2$ when moving to a point stable in these areas E_2.

Solutions of the system (3) corresponding to genetic divergence, lying in a single cube, can be expected to be found with reduced fitness of heterozygotes, that is, at $s < 0$. In this case, the parametric space turns out to consist of a larger number of regions, some of which are numbered (where there are stable points), and some with complex dynamics require separate consideration (in Fig. 2, *a* is denoted as *Chaos*). Let's first consider those that have a meaningful biological meaning and correspond to simple stable dynamics modes, namely those for which the selection coefficient of heterozygotes lies in the range $-1 \leqslant s < 0$.

In the area *5*, at the intersection of the line $m = -s/4$, a pair of fixed points E_3 and E_4 corresponding to genetic divergence is split off from the point E_2. They are located in a unit cube on the line $q_1 + q_2 = 1$, but they turn out to be unstable. In the *6* area, this pair disappears. In both cases, the fixed points E_0 and E_1 correspond to the monomorphic state of adjacent

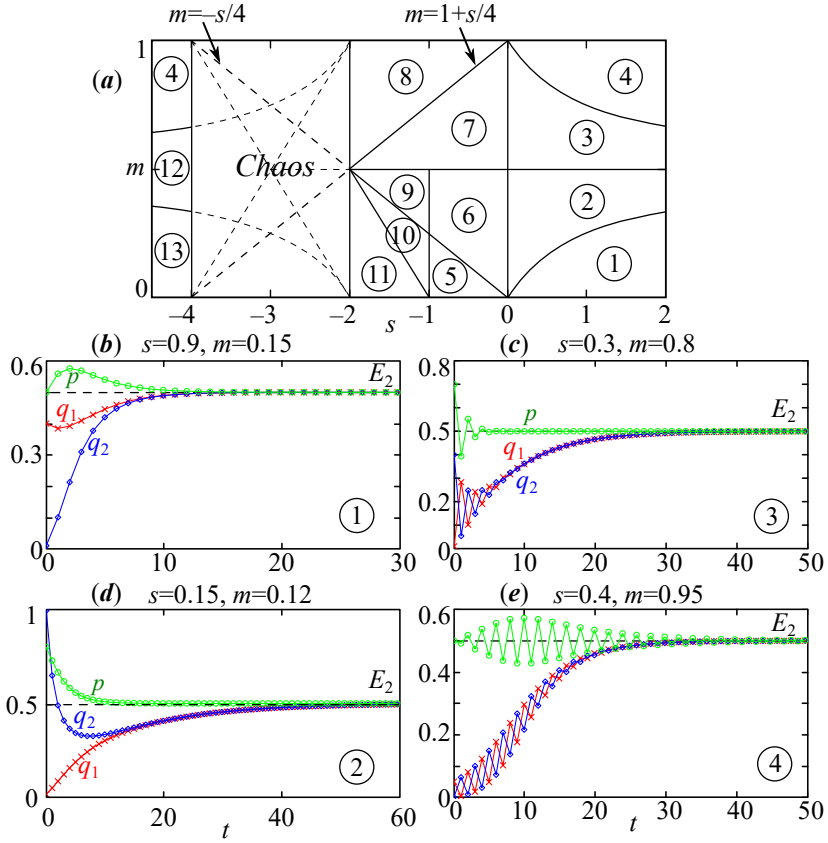

Fig. 2. *a* — Параметрический портрет системы (3), *b*–*e* — примеры динамики для параметров из областей *1*–*4* при $s > 0$ (цвет онлайн)

Fig. 2. *a* — Parametric portrait of the system (3) and *b*–*e* — examples of dynamics in the domains *1*–*4* (polymorphic state is stable) for $s > 0$ (color online)

populations, — stable. Therefore, the dynamics of the system (3) is bistable. The pools of their attraction, as already noted, are limited by the faces of a single cube and the separatrix surface W^S. If the starting point lies below W^S ($Q < 1/2$), individuals with only the aa genotype remain in both populations over time ($q_1 = 0$, $q_2 = 1$), if higher than W^S ($Q > 1/2$) — with genotype AA ($q_1 = 1$, $q_2 = 0$). However, the presence in the *5* region of even an unstable pair of points E_3 and E_4 significantly changes the nature of the transition to one of these monomorphic states. For example, for parameters from the area *6*, where there are no points E_3 and E_4, the transition to E_0 or E_1 is monotonous and corresponds to logistic growth (transition to E_1) or falling (to E_0). While in the *5* region, the presence of a pair of saddle points E_3 and E_4 leads to the fact that, under certain conditions , rather non-monotonic transient dynamics modes arise (Fig. 3, *a*). They arise if the trajectory passes in the vicinity of an unstable one-dimensional manifold starting from the point E_3 or E_4 and passing into a stable manifold of points E_0 or E_1 (heteroclinic contour W^U).

For parameters from the *7* and *8* regions, the points are also stable E_0 and E_1, and the pair E_3 and E_4 does not exist. As a result , stability of dynamics is also observed. But unlike the previous case , there are several features here.

First, similar to the areas *3* and *4*, two eigenvalues in points $E_0 - E_2$ become negative when $m > 0.5$. This means that sawtooth oscillations are formed in the vicinity of fixed points. It can be expected that when moving to one of the stable points (E_0 or E_1) , damping fluctuations occur. However, it is not difficult to show that not every perturbation or starting point leads to

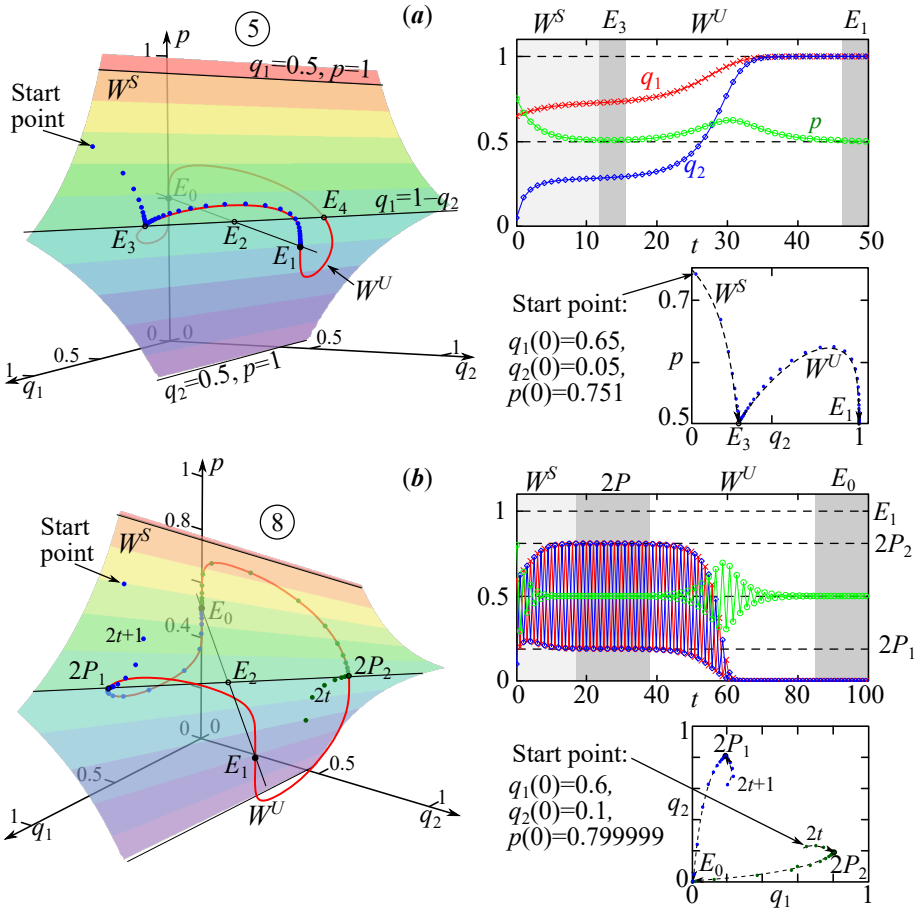

Fig. 3. Слева — фазовый портрет, справа — примеры динамики системы (3) для параметров из области *5* и *8* на рис. 2, *a* при *a* — $s = -0.5$, $m = 0.1$ и *b* — $s = -0.65$, $m = 0.9$ (цвет онлайн)

Fig. 3. Phase portrait (on the left) and examples of dynamics (3) (on the right) for parameters from domain *5* and *8* (monomorphic states are stable) at *a* — $s = -0.5$, $m = 0.1$ and *b* — $s = -0.65$, $m = 0.9$ (color online)

fluctuations, especially in variables q_1 and q_2. Such fluctuations occur only if the coordinates of the starting point the points are arranged symmetrically with respect to 1 or 0. For example, if $0 < q_1(0) < 1 < q_2(0)$ or $q_1(0) < 0 < q_2(0) < 1$, which contradicts the meaning of these phase variables. However, even if it is not $(0 < q_1(0) \leqslant q_2(0) < 1)$, and the variables q_1 and q_2 do not exhibit damped oscillations, then fluctuations may be present in the variable p. But only if $p(0) \neq 0.5$; and the more $p(0)$ differs from 0.5 (but does not come out of the unit cube), the greater the scope of fluctuations and the longer the transition process. At the same time, in the vicinity of the point E_2 located in the center of the unit cube, there are fluctuations in all three phase variables. The condition of their occurrence: $q_1(0) \neq q_2(0)$ and $p(0) \neq 0.5$. Since both negative eigenvalues at this point lie in a unit circle, and the third is greater than one, these fluctuations are quickly replaced by a monotonous rise or fall to point E_0 or E_1.

Secondly, in addition to the described dynamic behavior , a pair of saddle periodic points appears in the neighborhood of points $E_0 - E_2$ for parameters from the area *8* and in the display (3) . This pair splits off from E_2 at the intersection of the line $m = 1 + s/4$, and its appearance is accompanied by the exit of one of the negative eigenvalues from the unit circle. But since the third eigenvalue is still greater than one, the periodic point turns out to be unstable, that is, in this case there is a subcritical period doubling bifurcation. Let's denote a pair of these points by

$2P_{1,2}$. One of its coordinates is easy to calculate by putting $p = 0.5$, $q_1 = 1 - q_2$ and integrating the one-dimensional map twice:

$$q \mapsto \frac{m + (1 + s - 2m)q - sq^2}{1 + 2sq(1 - q)}.$$

As a result, the periodic point of the system (3) has the form:

$$2P_{1,2}\left(\frac{1}{2} \pm \frac{\sqrt{s(s - 4m + 4)}}{2s}, \frac{1}{2} \mp \frac{\sqrt{s(s - 4m + 4)}}{2s}, \frac{1}{2}\right).$$

These two points lie on the line $q_1 + q_2 = 1$ and, to some extent, «replace» the fixed points E_3 and E_4 missing in the area *8*, corresponding to the genetic divergence. It should be noted that the same pair of points exists at $s > 0$, but lies outside the limit of the unit cube.

As for fixed points, the corresponding eigenvalues of the Jacobi matrix calculated for a doubly iterated system (3) can be calculated for a periodic point. As a result, it is easy to see that in the *8* pair $2P_{1,2}$ — is a saddle with a one-dimensional unstable manifold that forms a heteroclinic contour W^U closed to stable points E_0 and E_1. Since all eigenvalues at points $2P_{1,2}$ are positive, the mapping (3) is orientable. Therefore, there is there are four contours, and from the points $2P_{1,2}$ you can come to both E_0 and E_1. As a result, the movement to stable points E_0 and E_1 for any initial conditions consists of two branches: for even t, the trajectory lies below the plane $p = 0.5$, for odd ones — higher, or vice versa, depending on where the starting point is located. As a result, there are fluctuations in all three variables, an example of which is shown in Fig. 3, *b*, where the starting point is located in the neighborhood of the manifold W^S. In this case, the trajectory first moves along the separatrix surface W^S towards the periodic point $2P$, where it «lingers» for a while, and then rushes to the point E_0 or E_1 along the two branches of the contour W^U. It should be noted that none the trajectory does not intersect the surface of W^S in this case.

Thus, with reduced fitness of heterozygotes, that is, at $-1 \leqslant s < 0$, genetic divergence is possible only as part of a transitional process, similar to how it happens in the continuous-time model [20]. Moreover, for $m < -s/4$, the solutions of continuous and discrete-time models coincide. However , at $m \geqslant 1 + s/4$, the discrete nature of reproduction leads to the transition to one from monomorphic states, it is accompanied by sawtooth oscillations when the ratio of the concentration of the A allele changes periodically in different populations, which in principle cannot be in a continuous-time model. It is quite expected that the pair of fixed points E_3 and E_4 corresponding to the divergence becomes stable at $m = 0$ when the two populations are unrelated and develop independently. Similar to the case of a continuous-time model [20] points E_3 and E_4 turn into straight lines of fixed points $(0, 1, \bar{p})$ and $(1, 0, \bar{p})$ ($\bar{p} \in R$ — any number). As a result, the concentrations of alleles at different sites in the asymptotic case take the values 0 or 1, while as their numbers, expressed in terms of weight p, take any values (depending on the initial conditions). Similar solutions of the system (3) corresponding to the divergence are observed at $m = 1$. In this case, a pair of periodic points $2P_{1,2}$ with coordinates $(0, 1, \bar{p})$ and $(1, 0, \bar{p})$ ($\bar{p} \in R$) is stable. As a result, the concentrations of alleles q_1 and q_2 fluctuate between 0 and 1 with opposite phases, and the range of fluctuations in the weight of p takes any value depending on its initial value.

Let's consider the features of dynamics at $s < -1$, when the system, at first glance, loses its meaningful meaning. On the one hand, at $-2 < s < -1$, the solutions, for the most part, lie in a unit cube. For example, for the *7* and *8* regions, the parameter values are s lie in the range $[-2; 0]$, and the above types of dynamics are observed there, and they do not have any features

that contradict the meaningful meaning of the problem. However, at $0 \leqslant m < 0.5$ there is a clear boundary $s = -1$ between the areas *6*–*7* and *9*–*11*. In the area of *9*, as in *6*, there are no points E_3 and E_4 corresponding to the divergence. The points E_0 and E_1 are still stable, but unlike the area *6*, all multipliers are positive. Therefore, only monotonous movement to one of these points is possible here.

When the line $m = -s/4$ intersects, a pair of points E_3 and E_4 appears, and two eigenvalues at points E_0 and E_1 turn out to be negative. In as a result, for parameters from the domain *10* and *11*, damping oscillations inevitably occur around the point E_0 or E_1, which always exit the unit cube under almost any initial conditions, except for the case when the starting point lies on the edges of the unit cube, that is, $\big(q_1(0), q_2(0), p(0)\big) = E_0$ or E_1 ($p(0)$ can be any). The area *10* differs from *11* only in that the two eigenvalues at the points E_3 and E_4 become negative.

2.2. Complex modes. Crossing the boundary of $s = -2$, that is, far beyond the limit of biologically significant parameters, complex chaotic oscillations are formed in the system (3) that go far beyond the limits of a single cube and lose their meaningful meaning. Despite this, we will briefly consider their features, since such dynamics may be of some interest to the theory of dynamical systems as an example of complexly organized oscillations.

On the line $s = -2$, the largest modulo eigenvalue for each fixed point is -1. As a result, a degenerate 2-cycle occurs around the points E_0, E_1 or E_2, the amplitude of which depends on the initial conditions and the value of m. U $s < -2$ this cycle breaks down and chaotic fluctuations occur. The features of their appearance and transformation can no longer be described by analyzing only the values of their own numbers.

In the case of complex dynamics, other criteria are needed. For example, it is not difficult to numerically determine Lyapunov exponents, and then estimate the dimension the attractor according to the Kaplan–York formula. The result can be supplemented with a map of dynamic modes. In Fig. 4, *a* the calculated indicators of the chaotic dynamics of the system (3) are shown, from which an important observation follows. At $-4 < s < -2$, the oscillation period of the variables $q_1(t)$ and $q_2(t)$ — always an unlimited quantity, that is, there is no limit $\lim\limits_{t\to\infty} \|q(t) - q(t+T)\| = 0$, $T \in \mathrm{N}$ (it is impossible to estimate the period T by the finite series of the solution of the system (3)). While the weight of $p(t)$ may not experience fluctuations at all in enough a wide band of parameters (the black bar on the right side of Fig. 4, *a*). In this range of parameters, after the transition process, $p(t)$ turns out to be equal to 0.5 (for $t \to \infty$). This is accompanied by a complete synchronization of the dynamics of the variables q_1 and q_2. As a result, the points of the trajectory lie on the line $q_1(t) = q_2(t)$, $p(t) = 0.5$ in the asymptotic case.

Numerical experiments show that if $p(0) \neq 0.5$, then the process of chaotic synchronization can be quite long, containing intermittent sections of partial synchronization and sections of non-synchronous dynamics. In addition, strong jumps of the variable are possible p against the background of seemingly well-established dynamics. As a result, the synchronous mode area on the dynamic mode map is slightly noisy single white dots inside, and the border is a little fuzzy, especially when s, close to -2 and -4. But the Lyapunov exponent and the dimension the attractors are insensitive to such phenomena due to averaging and clearly register the described boundary. Outside this band, under any initial conditions , the variable p begins to experience irregular fluctuations, q_1 and q_2 they turn out to be out of sync with each other, and the dynamics becomes hyperhaotic (with a positive sum of all Lyapunov exponents and a dimension estimate equal to 3). Closer to the border , modes in which synchronization is interspersed with non-synchronous behavior are still registered. When moving away from the boundary for both small and large m, the dynamics becomes completely out of sync. Fig. 4, *b* shows examples demonstrating such a transition. The location of the parameter values used in these examples is

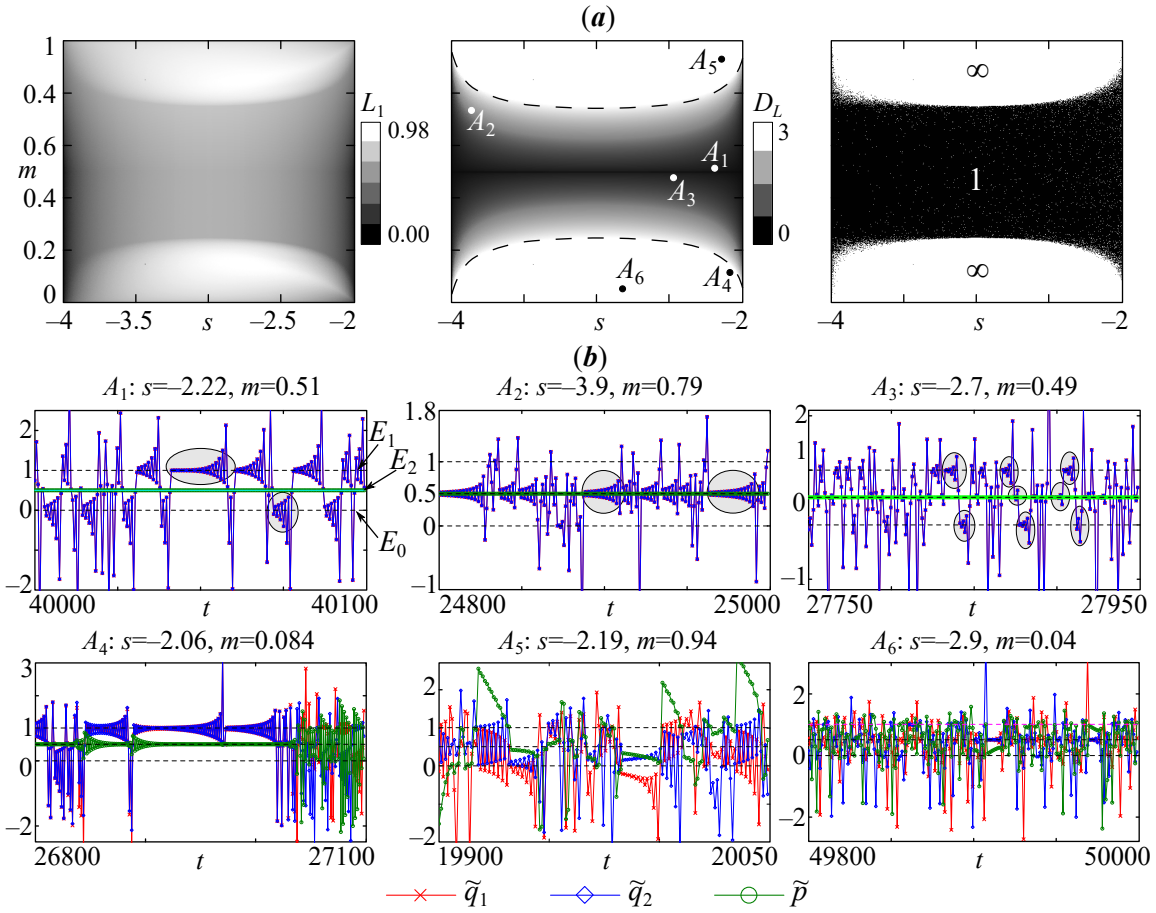

Fig. 4. *a* — On the left — the senior Lyapunov exponent (L_1), в центре — ляпуновская размерность (D_L), справа — период колебания фазовой переменной $p(t)$ (карта динамических режимов). *b* — Примеры синхронной (в точках A_1–A_3) и несинхронной (A_4–A_6) динамики системы (3) при указанных значениях параметров (цвет онлайн)

Fig. 4. *a* — Maximal Lyapunov exponent (L_1), Lyapunov dimension (D_L) and oscillation period of $p(t)$ (dynamic regimes chart). *b* — Examples of synchronous (at points A_1–A_3) and non-synchronous (A_4–A_6) dynamics of system (3) with the shown parameter values (color online)

marked with points A_i on the parametric plane (see Fig. 4, *a*).

The main feature of such complex dynamics modes is not so much in the alternation of synchronous and non-synchronous modes (intermittency) and the increase in the degree of randomization at a distance from the line $m = 0.5$, as in the structure of the chaotic a set that is quite clearly traceable. With a minimum degree of randomization ($m \sim 0.5$, $s \sim -2$), the dynamics of the system (3) can be represented as a repeating series of oscillations, which consists of alternating divergent oscillations around the points E_0 and E_1 with a quasi-random duration. So, in the first example (point A_1) ellipses highlight several long sections of such dynamics, which end with a sharp jump in the variables q_1 and q_2. After the jump trajectory passes into the vicinity of another fixed point, where divergent oscillations are formed again. Their duration, of course, is not random, but depends on how close to the fixed point after the jump turned out to be a trajectory. The closer, the longer the divergent ones last fluctuations. It is easy to see that the transition to the point E_0 occurs «bottom», that is, the trajectory goes into the area with negative coordinates, and the transition to E_1 occurs «from above», that is, from an area with very large coordinates. Apparently, there exist saddle periodic points generating separatrices

that do not allow unlimited trajectories. Indeed, several of them with small periods have been numerically detected (2, 3, 4).

It is important to emphasize that the jump in phase variables often turns out to be so large that it is difficult to depict the nature of oscillations on the linear scale of the coordinate axis . To solve this problem, you can scale the values of the phase variables according to the following rule. No scaling is applied for modulo small values of phase variables (for example, from -1.5 to 1.5). For large positive (greater than 1.5) or small negative values (less than -1.5) , logarithm is performed, preserving the sign of the scaled variable. In the result is a new variable that is used only for plotting the corresponding graphs (see Fig. 4 and 5), has the form:

$$\tilde{q}_i = \begin{cases} \ln(q_i) + 1.5, & \text{if } q_i > 1.5, \\ q_i, & \text{if } -1.5 \leqslant q_i \leqslant 1.5, \\ -\ln(-q_i) - 1.5, & \text{if } q_i < -1.5. \end{cases}$$

A similar scaling is performed for the variable p.

In the second example (point A_2), divergent oscillations with quasi-random duration are also observed, but mainly around a polymorphic point E_2. After several «turns» on the segment $0 \leqslant q_1(t) = q_2(t) \leqslant 1$ ($p(t) = 0.5$) the trajectory leaves the unit cube, reaching large absolute values, and then returns to the point E_2. But more interesting is the situation when the trajectory moves between three points E_0, E_1 and E_2, making several turns around each of them, the number of which is rarely large. Quasi-random in this case is not so much the duration divergent oscillations, how much is the point in the vicinity of which the trajectory will be after the jump of phase variables. In the first example in Fig. 4, *b* only one series of transitions is possible: $E_0 \to E_1 \to E_0 \to \ldots$, where the sign «$\to$» shows the transition of the trajectory from the neighborhood of one fixed point to another. In the second example, there are no transitions, and fluctuations are observed only around the point E_2. In the third example, there are significantly more options for the trajectory transition between three points. For example, transitions are possible $E_0 \to E_1 \to E_0 \to E_1 \to \ldots \to E_2 \to \ldots$ with rather rare traversals of the trajectory of the neighborhood of the point E_2, or on the contrary, frequent transitions $E_0 \to E_2 \to E_1 \to E_0 \to \ldots$ or $E_0 \to E_1 \to E_2 \to E_0 \to \ldots$, etc.,etc.

Finally, when the residence time is in the neighborhood of each of the fixed points becomes minimal (equal to 1-2 periods) the dynamics of the system (3) becomes truly unpredictable, although implemented on a one-dimensional manifold: $q_1 = q_2$, $p = 0.5$. In this case, the system (1) is represented as a one-dimensional mapping:

$$q \mapsto \frac{2q(1 + s(1 - q))}{2 + 4sq(1 - q)},$$

which has fixed points E_0, E_1 and E_2.

The exit from the synchronous dynamics area, as already noted, is accompanied by an intermittency of synchronous and non-synchronous dynamics sections, as in the fourth example in Fig. 4, *b* (A_4). At this moment , a series of transitions $E_0 \to E_0$ or $E_1 \to E_1$, separated by jumps of phase variables, are possible in synchronous sections. But it is more interesting that in this area, before completely losing synchronization, modes arise that contain sections of diverging or damping oscillations of variables q_1 and q_2, and are quite monotonous variable p (point A_5 in Fig. 4, *b*). In this case , the fluctuations of the variables q_1 and q_2 are antiphase, which converge (or diverge) to different values. This indicates that on a two-dimensional manifold, on which in this case implements all non-synchronous modes, there are saddle fixed (in addition to E_0, E_1 and E_2) or periodic points that attract the phase trajectory. Similarly to synchronous modes, transitions with strong jumps of variables occur between them.

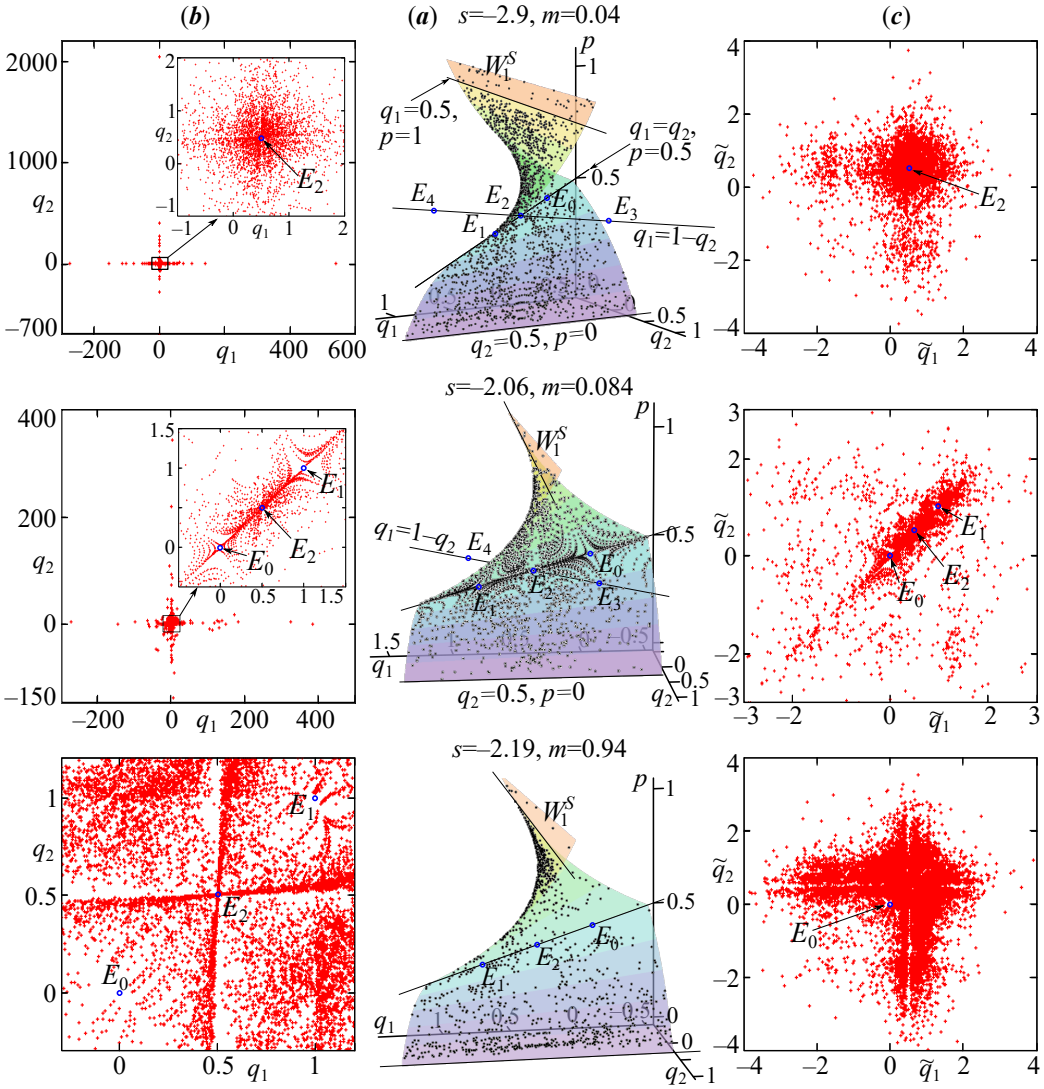

Fig. 5. Примеры гиперхаотической динамики системы (3) при указанных значениях параметров. *a* — Двумерное многообразие W_1^S с расположенными на нем фазовыми точками, а также их проекция на фазовую плоскость с естественными (*b*) и масштабированными (*c*) координатами (цвет онлайн)

Fig. 5. Examples of hyperchaotic dynamics (sum of all Lyapunov exponents is greater than zero) of system (3) for the shown parameters values. *a* — 2D manifold W_1^S with the orbit lying on it, and its projection onto the phase plane in natural (*b*) and scaled (*c*) coordinates (color online)

Finally, for small or large values of m, the dynamics of all variables turns out to be completely out of sync and hyperchaotic, as in the last example in Fig. 4, *b*.

Consider the value $Q'(t) = p(t)q_1(t) - \big(1 - p(t)\big)q_2(t) - p(t)$. Numerical calculations show that all complex dynamics modes lie on the surface given by the equation: $Q' = 1/2$. In addition, synchronous modes lie on a part of this surface (on a straight line $q_1(t) = q_2(t)$, $p(t) = 0.5$). Indeed, substituting in Q' the values of the phase variables corresponding to the established chaotic dynamics, we can make sure that the sum of the squares of the deviation of the phase trajectory from this surface does not exceed 10^{-9}, that is

$$\sum_{t=M}^{N} \Big(p(t)q_1(t) - \big(1 - p(t)\big)q_2(t) - p(t) - 0.5\Big)^2 \lesssim 10^{-9},$$

r$N > M$ — sufficiently large integers, $q_1(t)$, $q_2(t)$ and $p(t)$ — coordinates of the phase points of the system (3) at $-4 < s < -2$. It has not yet been possible to strictly prove the existence of this variety.

Let's denote the manifold defined by the equation $Q' = 1/2$ as W_1^S. It is easy to notice that W_1^S intersects with W^S along the following lines: $q_1 = 0.5$, $q_2 \in R$, $p = 1$; $q_1 \in R$, $q_2 = 0.5$, $p = 0$; $q_1 = q_2 = 0.5$, $p \in R$. In Fig. 5, *a* shows this surface with phase points lying on it in the case of hyperchaotic dynamics.

The right and left columns of Fig. 5 show that for different parameter values, the phase points of the system (3) inhomogeneously fill the manifold W_1^S. In the examples shown, the phase points are concentrated along the proper subspaces of the saddle points E_0 and E_1, and the chaotic set contains a fixed point E_2. This fact requires a separate thorough study.

3. Features of dynamics in the case of a constant number

Consider a situation in which populations in different territories remain constant in time or change synchronously. As a result , the ratio of the numbers $p = N_1/(N_1 + N_2)$ turns out to be a constant value, such that $0 < p < 1$. In this case, the system (3) has the form:

$$\begin{cases} q_1(t+1) = \dfrac{1}{G_1(t)}\left((1-m)q_1(t)\Big(1+s\big(1-q_1(t)\big)\Big) + m\dfrac{1-p}{p}q_2(t)\Big(1+s\big(1-q_2(t)\big)\Big)\right), \\ q_2(t+1) = \dfrac{1}{G_2(t)}\left((1-m)q_2(t)\Big(1+s\big(1-q_2(t)\big)\Big) + m\dfrac{p}{1-p}q_1(t)\Big(1+s\big(1-q_1(t)\big)\Big)\right), \end{cases} \tag{5}$$

where the normalization factors, as before, will be $G_1(t) = (1-m)(1+2sq_1(t)(1-q_1(t))) + m\frac{1-p}{p}(1+2sq_2(t)(1-q_2(t)))$ и $G_2(t) = (1-m)(1+2sq_2(t)(1-q_2(t))) + m\frac{p}{1-p}(1+2sq_1(t)(1-q_1(t)))$.

The mapping system (5) has from three to nine fixed points for different values of the parameters s, m and p . Analytically, in this case , only the first three points can be expressed, which always coincide with the points E_0, E_1 and E_2 systems (3) and always exist. The remaining points are only numerically found as the roots of a sixth-degree polynomial. This does not prevent us from determining that they appear either by splitting the points E_0, E_1 and E_2 for an additional pair of fixed points (fork bifurcation), or as a result of saddle-node bifurcation. In Fig. 6, *a*, *c* shows the specific boundaries of the birth of these fixed points, as well as the areas of their stability under variation of parameters. Below are shown the zero points of the system (5), the intersection points of which correspond to the fixed points of the system (5). The punctured point indicates that the fixed point is a saddle or unstable node (source), the bold point is a stable node (drain).

As in the general case (system (3)) with high fitness of heterozygotes, that is, $s > 0$, polymorphism is always established in the population (the point E_2 is stable). Variation of other parameters only changes the number of fixed points, the type of stability (saddles turn into unstable nodes or vice versa), as well as the mechanism of their birth. In Fig. 6, *a*, *c* areas of different colors (grayscale) correspond to the parameters at which a different number of fixed points exist in the system (5) . Accordingly , when crossing their borders , they are born or some of the dots disappear. So, fig. 6, *b* shows, for example, that when moving from the area B to A, from the points E_3 and E_4 is simultaneously split off two pairs of dots. Moreover, in such a way that the point E_3 or E_4 lies between them, at an equal distance from them. But this happens only with a large value of the migration coefficient $m > 0.5$ and $p = 0.5$. In general, $p \neq 0.5$ additional pairs of points appear as a result of saddle-node bifurcation away from the points E_3 and E_4. Similar thus, when $p = 0.5$ and the transition from the region B to C generates one

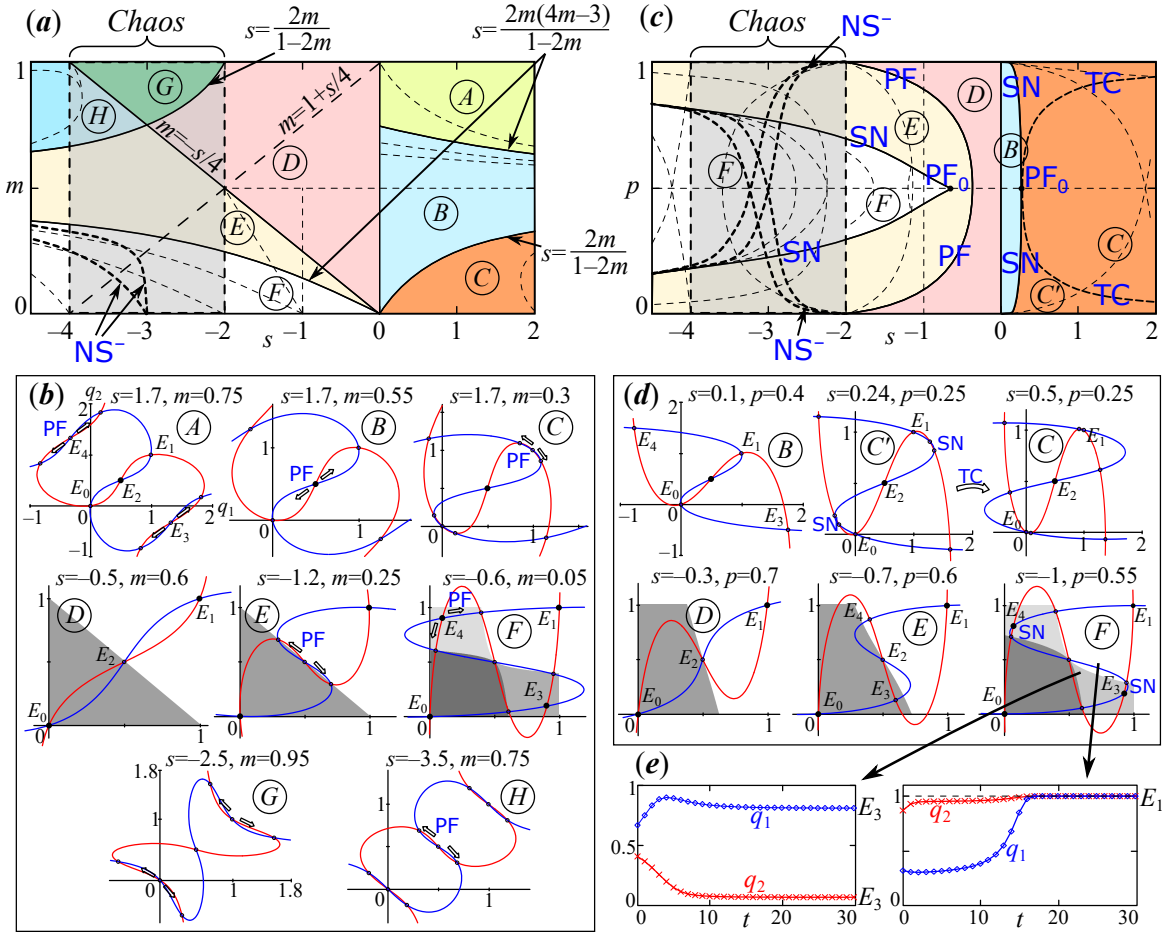

Fig. 6. *a*, *c* — Параметрический портрет с выделенной областью хаотической динамики (*Chaos*). *b*, *d* — Нульклины системы (5), показывающие число и расположение неподвижных точек в разных областях параметрического пространства. Нульклины совмещены с бассейнами притяжения би- и квадростабильных режимов. *e* — Пример динамики в случае квадростабильности. Использованы следующие значения параметров: *a*, *b* — $p = 0.5$ и *c*, *d*, *e* — $m = 0.1$, остальные значения указаны на рисунке (цвет онлайн)

Fig. 6. *a*, *c* — Parametric portrait (bifurcation diagram) with highlighted area of chaotic dynamics (*Chaos*). *b*, *d* — Nullclines of system (5), showing the number and location of fixed points in different regions of the parametric space, are combined with attraction basins of bi- and quadstable regimes. *e* — Examples of dynamics in the case of quadstability (two divergent and two monomorphic states are stable). The following parameter values have been used: *a*, *b* — $p = 0.5$ and *c*, *d*, *e* — $m = 0.1$, other values are shown in the figure (color online)

pair of points around the polymorphic point E_2. At $p \neq 0.5$, it appears as a result of saddle-node bifurcation (see Fig. 6, *c*). Similarly to the system (3), at high values of the migration parameter $m > 0.5$, part of the eigenvalues turns out to be negative (including for the stable point E_2). As a result, the movement towards a stable polymorphic point E_2 under certain initial conditions is accompanied by damping fluctuations of the phase variables q_1 and q_2. Here you can explain, that the dotted lines in Fig. 6, *a*, *c* show the parameters at which the real part of the eigenvalues changes its sign or they are located on a unit circle. That is, when these lines intersect in the system (5) , certain qualitative changes occur, which, at $s > 0$, although they do not affect the stability of the point E_2, but significantly change the nature of the transition dynamics. In general, the dynamics modes here are similar to those marked for the complete system (3).

With low fitness of heterozygotes ($s < 0$), bistability of dynamics is observed. In this case, the points E_0 and E_1, which also existed at $s > 0$, acquire stability when moving from

the regions A, B or E to the region of parameters D, that is, at $-2 < s < 0$ and $0 < p < 1$. At the same time, with a relatively low migration coefficient in the system (5), four points are already stable. This happens when moving to the F area. In this case, we can say that the system (5) becomes quadrostable, and a stable one is possible in a system of two populations genetic divergence (fig. 6, *e*). This is made possible by additional bifurcation. Strictly at $p = 0.5$ on the border between E and F a pair of unstable points is split off from the saddle points E_3 and E_4, and E_3 themselves and E_4, on the contrary, acquire stability (Fig. 6, *b*). At $p \neq 0.5$, the points E_3 and E_4 are always unstable, and the additional two pairs of stable and unstable points (saddle and node) appear away from them (fig. 6, *d*). However, in the future they may experience transcritical a bifurcation and a stable point will appear between the two saddles, although not so symmetrically as in the case of $p = 1/2$. For more information about this bifurcation in the case of a continuous -time model, see [20]. It is important to note here that the more the value of the parameter p differs from $1/2$, the lower the values of s this bifurcation occurs (the appearance of quadrostable modes) (see Fig. 6, *c*). In addition, the growth of the migration coefficient m «pushes» this border closer to the chaotic region dynamics whose boundaries do not depend on m and p. As a result , at high values m fixed points corresponding to genetic divergence (E_3 and E_4) turn out to be unstable or do not exist, and outside the chaotic dynamics region ($-2 < s < 0$) only monomorphic points E_0 and E_1 corresponding to the monomorphic state of populations are stable.

At high values of the migration parameter m , periodic points of period 2 appear instead of missing points corresponding to divergence, which again make the model (5) quadrostable in a certain sense. For $p = 1/2$, one of these pairs coincides with the point $2P_{1,2}$ found for the system (3). With such a weight value p, it is possible to accurately determine the range of parameters of the birth of these points and specify the area of their stability. It exists and has positive coordinates at $4(m - 1) < s < 0$. Its appearance is associated with subcritical the bifurcation of doubling the period of the point E_2 at the intersection of the line PD^- and the transition of parameters from the domain D to D' (Fig. 7, *a*). By $-2 < s < 2(1 - m)(4m - 1)/(1 - 2m)$ and $m > 0.5$ the pair of points $2P_{1,2}$ turns out to be stable. At the moment of crossing the PF line and moving from the D' area to D", from it a pair of saddle points is split off, and the points $2P_{1,2}$ acquire stability. At this moment, from the pool of attraction points E_0 and E_1 (on the left in Fig. 7, *b*) two regions of attraction of points are separated $2P_{1,2}$ (on the right in Fig. 7, *b*). The size of these areas increases as the migration coefficient increases and the distances between saddle points increase.

The appearance of a pair of periodic points $2P_{1,2}$ indicates that in the system of two related populations with low fitness of heterozygotes, genetic divergence is possible not only with a low migration coefficient, and not only as part of the transitional dynamics. This becomes possible if the ratio of numbers is preserved ($p = const$). However, unlike the case of weak migration, divergence in this case manifests itself in the form of periodic fluctuations between two states that they also coexist with two stable monomophic states of the population (E_0 or E_1). These fluctuations are manifested in the fact that the concentrations of the A allele at different sites experience periodic antiphase fluctuations with a period of 2 between states with a high concentration of the A allele in the first territory and a low concentration of the a allele in the second territory or vice versa. If at the same time a couple there are points $2P_{1,2}$, but it is not stable yet (in the range of parameters D'), then genetic divergence in the form of fluctuations can be observed only as part of transition process under specially selected initial conditions. An example of such dynamics is shown on the left in Fig. 7, *c* and is generally similar to the dynamics in Fig. 3, *b*. In this case, the starting point is chosen close to the separatrix $q_2 = 1 - q_1$. However, with a sufficiently large migration coefficient (the D" region), these fluctuations turn out to be

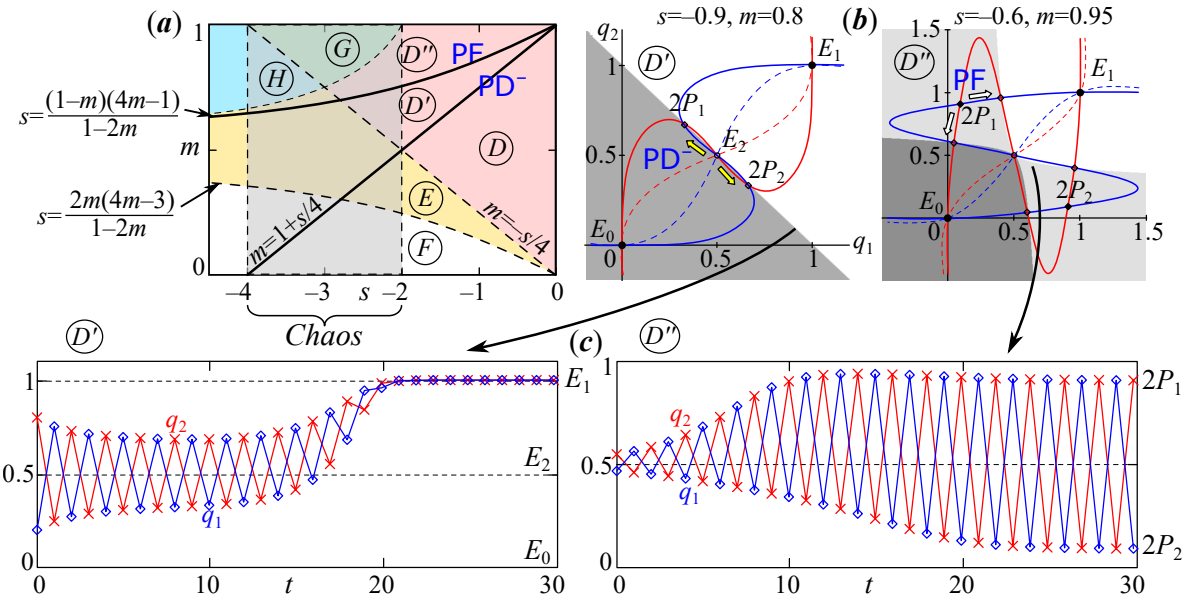

Fig. 7. *a* — Параметрический портрет системы (5) при $p = 0.5$ с нанесенной на него линией субкритической бифуркации удвоения периода PD$^-$ и последующей бифуркации вил PF, после которой периодическая точка $2P_{1,2}$ (2-цикл) приобретает устойчивость. *b* — Нульклины системы (5) (пунктирная линия) и второй итерации системы (5) (сплошная), а также бассейны притяжения устойчивых точек E_0, E_1 и $2P_{1,2}$. *c* — Примеры динамики в случае би- (слева) и квадростабильности (справа). Начало стрелки показывает примерное расположение стартовой точки (цвет онлайн)

Fig. 7. *a* — Parametric portrait of system (5) at $p = 0.5$ with a line of subcritical period doubling bifurcation PD$^-$ and subsequent supercritical pitchfork bifurcation PF after which the periodic point $2P_{1,2}$ (2-cycle) becomes stable. *b* — Nullclines of system (5) (dotted line) and second iteration of (5) (solid) as well as the attraction basins of stable points E_0, E_1 and $2P_{1,2}$. *c* — Examples of dynamics in the case of bi- (left) and quadstability (right). The arrow start shows the location of the starting point (color online)

stable and are observed for an unlimited time (the example on the right in Fig. 7, *b*). Interestingly, at lower values of the selection coefficient of heterozygotes s divergence possible with a lower coupling coefficient. However, crossing the border at $s < -1$ stable periodic points $2P_{1,2}$ come out of the unit square and the system (5), like the complete system (3), loses its meaningful meaning.

In the general case $p \neq 1/2$, the described scenario of the birth of a stable periodic regime does not change qualitatively. As the weight value p moves away from 0.5, the points $2P_{1,2}$ and the saddles surrounding them turn out to be located less symmetrically. As a result, the amplitude of fluctuations in the concentrations of the A allele at different sites turns out to be different (more where the number is smaller). In addition, the bifurcation lines PD$^-$ and PF are shifted higher, that is, a 2-cycle occurs at even higher values of m as the difference grows $|p - 0.5|$.

In the field of chaotic dynamics, these periodic points also exist, but are unstable. In addition, in the system (5), these points also exist when $s > 0$, however, they lie outside the first quadrant and are always unstable.

The properties of the chaotic dynamics of the system (3) and (5) are generally similar. However, in addition to synchronous (at high and low p) and absolutely non-synchronous chaotic modes (at p close to 0.5), the system (5) it also demonstrates antiphase chaotic fluctuations of the variables q_1 and q_2. In any case, the dynamics consists of sections of divergent oscillations around the points E_0, E_1 and E_2 with quasi-random duration, as for the model (3).

Other features of the system (5) include the appearance of nine fixed points at high values of $m > 0.5$ and $s < -2$. Their appearance is associated with a sequence of «doubling» points E_0, E_1 and E_2, which was not observed in the model (3). In the area of G, a pair of points it

splits off from the points E_0 and E_1, and in the area of H also from E_2. It is also true here that at $p = 0.5$ these additional points are born due to fork bifurcation (PF), and at $p \neq 0.5$ due to saddle-node bifurcation (SN). However among these additional points, there are never stable ones. Only leaving the area of chaotic dynamics (at $s < -4$), out of nine fixed points the polymorphic point E_2 becomes stable (the leftmost part of the diagram in Fig. 6, *a*, *c*).

Another feature of the system (5) is related to the fact that the lines of local bifurcations of the system (5), in general, similar to the bifurcations of the complete system (3) or a similar continuous-time model [20], several boundaries are added, on which part of the eigenvalues — are complex conjugate quantities. However, they exist only in the field of chaotic dynamics (*Chaos* in Fig. 6, *a*, *c*) at $-4 < s < -2$ and $0 < p < 1$. In Fig. 6, *a*, *c* these lines are indicated by the symbol NS^-, where the sign «–» indicates that only unstable points that appear together with points corresponding to genetic divergence are subject to this bifurcation. Therefore, it is quite difficult to judge changes in dynamics, related to these points, especially in the field of chaotic dynamics.

Conclusion

In this paper, the simplest model of primary genetic divergence in the system of two related panmictic populations with non-overlapping generations and a clear stage of development was considered. Unlike most similar works devoted to the search for conditions for the preservation of polymorphism, divergence and geographical variability [7, 10, 11, 18], the most complete model is considered, taking into account both the frequencies of alleles and the number of related populations. Specific bifurcations are indicated by modern methods of analysis of dynamic systems, which lead to divergence. Bifurcation diagrams, phase portraits and pools of attraction are constructed. Based on the analogue of saddle maps , the following classification of regions in the parameter space that differ in the type of dynamics (including transient dynamics).

The discrete representation of time in the model leads to some differences from the similar model with continuous time, which we considered earlier [20]. For small values of the migration coefficient ($m < 0.5$) , bifurcation lines coincide, on which solutions corresponding to divergence are born. The solutions in this case are qualitatively equivalent. Significant differences are observed at high values of the migration coefficient ($m > 0.5$), when under certain conditions there are fluctuations in the frequencies of alleles or the ratio of numbers.

Modes corresponding to divergence are possible with reduced fitness of heterozygotes, when the dynamics turns out to be bistable or even quadrostable. In the case of bistability, divergence is possible only as part of the transition process if the corresponding divergences of the solution exist, but are not yet stable (although bistability is possible without the existence of this additional solution). The stabilization of the divergent state occurs under certain restrictions imposed on the growth of the population. For example, with the introduction of ecological limitation of population growth. The emergence of a stable genetic divergence is accompanied by a number of qualitative rearrangements. With a weak connection, subcritical fork bifurcation of a polymorphic fixed point occurs, followed by supercritical fork bifurcation (in the case of equal numbers in both territories), or saddle-node bifurcation (with unequal numbers). With a strong connection , the scenario similar, however, instead of subcritical bifurcation of a polymorphic fixed point, a subcritical doubling of the period occurs, and the subsequent bifurcation generates a stable periodic point (2-cycle). In this case, the dynamics turns out to be quadrostable — depending on the initial genetic structure, both populations turn out to be genetically homogeneous (monomorphism), or they show significant differences in structure (divergence). At high values of the migration coefficient, divergence is accompanied by antiphase fluctuations in allele frequencies in different territories.

Complex dynamic modes have been discovered, which, although they do not have a meaningful biological meaning, may be interesting as an example. complexly organized dynamics. Their peculiarity consists in a series of divergent oscillations around different fixed points corresponding to monomorphism or polymorphism in adjacent populations, and quasi-random transitions between them.

References

1. Haldane JBS. A mathematical theory of natural and artificial selection. Part II. The influence of partial self-fertilisation, inbreeding, assortative mating, and selective fertilisation on the composition of Mendelian populations, and on natural selection. Biological Reviews. 1924;1(3):158–163. DOI: 10.1111/j.1469-185X.1924.tb00546.x.
2. Fisher RA. The Genetical Theory of Natural Selection. Oxford: Clarendon Press; 1930. 272 p. DOI: 10.5962/bhl.title.27468.
3. Wright S. Evolution in Mendelian populations. Genetics. 1931;16(2):97–159. DOI: 10.1093/genetics/16.2.97.
4. Frisman EY, Shapiro AP. Selected Mathematical Models of Divergent Evolution of Populations. Moscow: Nauka; 1977. 152 p. (in Russian).
5. Svirezhev YM, Pasekov VP. Fundamentals of Mathematical Genetics. Moscow: Nauka; 1982. 512 p. (in Russian).
6. Frisman EY. Primary Genetic Divergence (Theoretical Analysis and Modeling). Vladivostok: FESC AS USSR; 1986. 160 p. (in Russian).
7. Bürger R. A survey of migration-selection models in population genetics. Discrete & Continuous Dynamical Systems - B. 2014;19(4):883–959. DOI: 10.3934/dcdsb.2014.19.883.
8. Carroll SP, Hendry AP, Reznick DN, Fox CW. Evolution on ecological time-scales. Functional Ecology. 2007;21(3):387–393. DOI: 10.1111/j.1365-2435.2007.01289.x.
9. Pelletier F, Garant D, Hendry AP. Eco-evolutionary dynamics. Phil. Trans. R. Soc. B. 2009; 364(1523):1483–1489. DOI: 10.1098/rstb.2009.0027.
10. Yeaman S, Otto SP. Establishment and maintenance of adaptive genetic divergence under migration, selection, and drift. Evolution. 2011;65(7):2123–2129. DOI: 10.1111/j.1558-5646.2011.01277.x.
11. Bertram J, Masel J. Different mechanisms drive the maintenance of polymorphism at loci subject to strong versus weak fluctuating selection. Evolution. 2019;73(5):883–896. DOI: 10.1111/evo.13719.
12. Neverova GP, Zhdanova OL, Frisman EY. Effects of natural selection by fertility on the evolution of the dynamic modes of population number: bistability and multistability. Nonlinear Dyn. 2020;101(1):687–709. DOI: 10.1007/s11071-020-05745-w.
13. Zhdanova OL, Frisman EY. Genetic polymorphism under cyclical selection in long-lived species: The complex effect of age structure and maternal selection. Journal of Theoretical Biology. 2021;512:110564. DOI: 10.1016/j.jtbi.2020.110564.
14. Telschow A, Hammerstein P, Werren JH. The effect of Wolbachia on genetic divergence between populations: Models with two-way migration. The American Naturalist. 2002;160(S4):S54–S66. DOI: 10.1086/342153.
15. Fussmann GF, Loreau M, Abrams PA. Eco-evolutionary dynamics of communities and ecosystems. Functional Ecology. 2007;21(3):465–477. DOI: 10.1111/j.1365-2435.2007.01275.x.
16. Tellier A, Brown JKM. Stability of genetic polymorphism in host–parasite interactions. Proc. R. Soc. B. 2007;274(1611):809–817. DOI: 10.1098/rspb.2006.0281.
17. Nagylaki T, Lou Y. The dynamics of migration–selection models. In: Friedman A, editor.

Tutorials in Mathematical Biosciences IV. Vol. 1922 of Lecture Notes in Mathematics. Berlin, Heidelberg: Springer; 2008. P. 117–170. DOI: 10.1007/978-3-540-74331-6_4.
18. Akerman A, Bürger R. The consequences of gene flow for local adaptation and differentiation: a two-locus two-deme model. J. Math. Biol. 2014;68(5):1135–1198. DOI: 10.1007/s00285-013-0660-z.
19. Passekov VP. On the analysis of weak two-locus viability selection and quasi-linkage equilibrium. Dokl. Biol. Sci. 2019;484(1):23–26. DOI: 10.1134/S0012496619010071.
20. Frisman EJ, Kulakov MP. On the genetic divergence of two adjacent populations living in a homogeneous habitat. Izvestiya VUZ. Applied Nonlinear Dynamics. 2021;29(5):706–726 (in Russian). DOI: 10.18500/0869-6632-2021-29-5-706-726.
21. Frisman EY, Zhdanova OL, Kulakov MP, Neverova GP, Revutskaya OL. Mathematical modeling of population dynamics based on recurrent equations: Results and prospects. Part II. Biology Bulletin. 2021;48(3):239–250. DOI: 10.1134/S1062359021030055.
22. Altrock PM, Traulsen A, Reeves RG, Reed FA. Using underdominance to bi-stably transform local populations. Journal of Theoretical Biology. 2010;267(1):62–75. DOI: 10.1016/j.jtbi.2010.08.004.
23. Láruson ÁJ, Reed FA. Stability of underdominant genetic polymorphisms in population networks. Journal of Theoretical Biology. 2016;390:156–163. DOI: 10.1016/j.jtbi.2015.11.023.
24. Gonchenko AS, Gonchenko SV, Kazakov AO, Kozlov AD. Mathematical theory of dynamical chaos and its applications: review part 1. Pseudohyperbolic attractors. Izvestiya VUZ. Applied Nonlinear Dynamics. 2017;25(2):4–36. DOI: 10.18500/0869-6632-2017-25-2-4-36.